Journal of Power Sources 268 (2014) 129–136

Contents lists available at ScienceDirect

Journal of Power Sources

journal homepage: www.elsevier.com/locate/jpowsour

Investigation of PdIr/C electrocatalysts as anode on the performance of direct ammonia fuel cell

M.H.M.T. Assumpção [a], S.G. da Silva [a], R.F.B. De Souza [a], G.S. Buzzo [a], E.V. Spinacé [a], M.C. Santos [b], A.O. Neto [a], J.C.M. Silva [a, *]

[a] Instituto de Pesquisas Energéticas e Nucleares, IPEN/CNEN-SP, Av. Prof. Lineu Prestes, 2242 Cidade Universitária, CEP 05508-900, São Paulo, SP, Brazil
[b] Laboratório de Eletroquímica e Materiais Nanoestruturados, Centro de Ciências Naturais e Humanas, Universidade Federal do ABC, Rua Santa Adélia, 166, CEP 09210-170, Santo André, SP, Brazil

HIGHLIGHTS

- Direct ammonia fuel cell (DAFC) performance using PdIr/C electrocatalysts as anode.
- A study of different NH_4OH concentrations at different fuel cell temperatures.
- Using PdIr/C 30:70 were obtained the highest power density and open circuit voltage.

ARTICLE INFO

Article history:
Received 11 March 2014
Received in revised form
3 June 2014
Accepted 4 June 2014
Available online 12 June 2014

Keywords:
Direct ammonia fuel cell
PdIr/C electrocatalysts
Nanoparticles
Electrochemical experiments

ABSTRACT

This work investigates the ammonia electro-oxidation considering electrochemical and direct ammonia fuel cell (DAFC) experiments. The working electrodes/anodes are composed of Pd/C, PdIr/C (90:10, 70:30, 50:50, 30:70 and 10:90 atomic ratios) and Ir/C. Solutions of 1 mol L^{-1} NH_4OH and 1 mol L^{-1} KOH were used for electrochemical experiments while 1.0, 3.0 and 5.0 mol L^{-1} NH_4OH in 1.0 mol L^{-1} KOH were used in DAFC. X-ray diffraction analysis of PdIr/C electrocatalysts suggests the formation of PdIr alloy, while transmission electron micrographs show the average particle diameters between 4.6 and 6.2 nm. Electrochemical experiments indicate PdIr/C 30:70 as the best electrocatalyst in accordance with DAFC. The maximum power densities obtained with PdIr/C 30:70 as anode using 5 mol L^{-1} NH_4OH and 1 mol L^{-1} KOH at 40 °C are 60% and 30% higher than the ones obtained with Pd/C and Ir/C electrocatalysts, respectively. The enhanced synergic effect in this specific composition may be assigned to an optimal ratio of palladium sites that dehydrogenates ammonia at lower overpotential with the lower surface coverage of N_{ads} on iridium. Furthermore, electronic effect between palladium and iridium might also contribute to the decrease of poisoning on catalyst surface by N_{ads}.

1. Introduction

The excessive use of fossil fuels has resulted in harmful effects on human health and welfare as well as the environment [1]. In this context, fuel cells may offer an excellent alternative to the current energy generation as a clean and efficient power source [2]. Fuel cells are attractive devices to obtain electric energy directly from the oxidation of hydrogen and other fuels in stationary and portable applications. Liquid fuels are considerably more convenient in terms of easy handling than gaseous hydrogen [3].

From both, an energetic and ecological point of view, ammonia has been considered as a potential fuel for direct alkaline fuel cells, since ammonia is easy to handle and to transport as a liquid or as a concentrated aqueous solution, it is easy in liquefaction at ambient temperature and has low production cost, (roughly US$ 1.2 kW h^{-1}), for comparison, methanol costs US$ 3.8 kW h^{-1} and hydrogen US$ 25.4 kW h^{-1} [4–6]. Moreover, ammonia is a carbon-free chemical energy carrier. The hydrogen storage capacity (17.7 wt%) and the theoretical charge for ammonia oxidation to N_2 is 4.75 Ah g^{-1} that compares very well with the theoretical charge of methanol in its oxidation to CO_2, 5.02 Ah g^{-1} [5,6]. Furthermore, liquid ammonia has 70% more hydrogen content and 50% higher specific energy density than liquid hydrogen per unit volume [7].

However, the main drawback of ammonia is its toxicity, but it is self alarming and any leakage can be detected by nose in

* Corresponding author. Tel.: +55 11 3133 9284; fax: +55 11 3133 9285.
E-mail addresses: quimijulio@gmail.com, quimijulio@yahoo.com.br (J.C.M. Silva).

http://dx.doi.org/10.1016/j.jpowsour.2014.06.025
0378-7753/

concentrations as low as 5 ppm, and due to its lower density than the air if escapes into the atmosphere ammonia dissipates rapidly [1].

Several studies about ammonia electro-oxidation reaction in alkaline media have been reported [6–10], and transitions noble metals such as Pt, Rh, Pd and Ir have been shown to be active for this reaction [7,10]. Considering this process, Pt is the most active metal to improve the kinetics of ammonia electro–oxidation reaction [6,11]. However, because of its elevated cost and limited resources, Pt cannot be used for large-scale applications. Additionally, Pt is easily poisoned by N_{ads} species [8]. Zhong et al. [6] reported that Pt and Ir are the most active metals for ammonia electro-oxidation. According to the authors, the dehydrogenation of ammonia on Ir occurs at lower potential and faster kinetic than on Pt. An important point of using Ir electrode is that it has lower overpotential of ammonia electro-oxidation (0.35 V *vs.* RHE) than Pt (0.43 V *vs.* RHE) in 0.1 mol L^{-1} NH_3 and 1 mol L^{-1} KOH [7]. Furthermore, Ir is about 35% cheaper than Pt [12].

Pd is another choice as a metal for ammonia electro-oxidation, since the electro–catalytic activity for the ammonia electro-oxidation varied in the increasing order of Ru < Rh < Pd < Ir < Pt. This order in catalytic activity reflected the difference in the affinity of N_{ad} for the metal surface [4]. The N_{ads}-Pd binding energy is higher than N_{ads}-Ir and N_{ads}-Pt, this phenomenon leads to the formation of a poisonous surface by nitrogen adsorbed at lower potentials than on Pt and Ir [6]. However, PtPd/C has higher catalytic activity towards ammonia oxidation than carbon-supported Pt [5,8]. Furthermore, Pd is about 57% cheaper than Pt [12].

It is important to point out that just few studies contemplate the real conditions of the cell operation at low temperature when the issue is the use of ammonia as fuel. The literature cited above take into account just electrochemistry experiments. Using a DAFC operated at 50 °C and Pt/C, Ru/C and PtRu/C as anode electrocatalysts, Suzuki et al. [4] reported that the open circuit voltage potential is dependent on the catalysts compositions, and it has been achieved 0.54 V using PtRu/C, 0.37 V using Pt/C and 0.08 V using Ru/C, values below the theoretical one of 1.17 V. Lan and Tao [13] also reported the results of a DAFC and from this study it was indicated that the best results were obtained using NH_4OH aqueous solution compared to NH_3 gas.

Recently, we have investigated the DAFC performance at 40 °C using Pt/C, Ir/C and PtIr/C as anode electrocatalysts [14] and we showed that among the PtIr/C compositions and NH_4OH concentrations, PtIr/C 50:50 (atomic ratios) electrocatalyst and NH_4OH 5.0 mol L^{-1} in KOH 1.0 mol L^{-1} showed the best result. In this work, the maximum power density obtained was 48% and 70% higher than that obtained using Pt/C and Ir/C electrocatalysts, respectively.

Aiming the development of DAFCs, the present study describes not only electrochemical but also DAFC experiments. This work describes the investigation of different compositions of PdIr/C as anode electrocatalysts, different NH_4OH concentrations in 1 mol L^{-1} KOH as a fuel and also two different temperatures, 40 °C and 50 °C of DAFC operation. For comparison, Pd/C and Ir/C were also evaluated as anodes. The stability of the materials were also evaluated by chronoamperometric experiments. The main characteristic of this study is the developing of Pt-free electrocatalysts for ammonia electro-oxidation, which is an important approach for the significant cost reduction of the electrocatalysts, thus contributing to its application on a technological scale.

2. Experimental

PdIr/C electrocatalysts (20 wt% of metals loading) with Pd:Ir atomic ratios of 90:10, 70:30, 50:50, 30:70, 10:90 and Ir/C and also Pd/C (20 wt% metal loading) were prepared by the borohydride reduction process [15,16] using $Pd(NO_3)_2.2H_2O$ (Sigma–Aldrich) and $IrCl_3.xH_2O$ 99.8% (Sigma–Aldrich), as metal sources. In this process Vulcan XC72 was firstly dispersed in an isopropyl alcohol/water solution (50/50, v/v). The mixture was homogenized under stirring and then the metals added and put on an ultrasonic bath for 5 min. After that, a solution of $NaBH_4$ in 0.1 mol L^{-1} KOH was added in one portion under stirring at room temperature and the resulting solution was maintained under stirring for 15 min more. After this, the final mixture was filtered and the solids washed with water and then dried at 70 °C for 2 h.

The electrocatalysts were characterized by X-ray diffraction (XRD) using a Rigaku diffractometer model Miniflex II using Cu Kα radiation source (0.15406 nm). The X-ray diffraction patterns were recorded in the range of $2\theta = 20°–90°$ with a step size of 0.05° and a scan time of 2 s per step. The atomic ratios of Pd and Ir in the synthesized materials were measured by energy dispersive spectroscopy (EDS) by using a JEOL – JSM6010 LA equipment.

Transmission electron microscopy (TEM) images were also carried out using a JEOL transmission electron microscope model JEM-2100 operated at 200 kV in order to obtain the morphology, distribution and nanoparticles size which were determined by counting about 100 particles at different regions of the different electrocatalysts [17–19].

Electrochemical measurements were performed at room temperature using a potentiostat/galvanostat PGSTAT 302N Autolab. A conventional three-electrode electrochemical cell was used. A platinum electrode and an Hg/HgO were used as the counter and reference electrodes, respectively. Glassy carbon (GC) electrodes were employed as support for the working electrodes (0.166 cm^2 of geometric area). Before each experiment, the GC support was polished with alumina suspension (1 μm) and washed in water. Ultrapure water obtained from a Milli-Q system (Millipore®) was used in all experimental procedures.

The working electrodes were constructed by dispersing 8 mg of the electrocatalyst powder in 1 mL water and mixing for 15 min in an ultrasonic bath. Shortly thereafter, 20 μL of 5% Nafion® solution was added to the suspension, which was mixed again for 20 min in an ultrasonic bath. Aliquots of 16 μL of the dispersion fluid were pipetted onto the GC surface. Finally, the electrode was dried at 60 °C for 20 min and hydrated for 2 min in water. All the electrochemical measurements were performed in a 1 mol L^{-1} KOH solution.

Cyclic voltammograms (CV) were carried out at a scan rate of 20 mV s^{-1} between −0.85 and 0.2 V vs. Hg/HgO. The electrocatalysts were cycled for five consecutive cycles resulting in the stable and reproducible shape of the voltammogram in ammonia free solutions and three consecutive cycles in ammonia containing solutions. Chronoamperometric experiments were carried out for 5 h at −0.35 V vs. Hg/HgO. The electro-oxidation of ammonia was performed in a 1 mol L^{-1} KOH and 1 mol L^{-1} NH_4OH solution.

The DAFCs experiments took place in a single cell with an area of 5 cm^2. The temperature was set to 40 °C and 50 °C for the fuel cell and 85 °C for the oxygen humidifier. All electrodes contained 2 mg of metal per cm^2 in the anode or in the cathode. In all experiments, commercial Pt/C from BASF was used in the cathode. The electrocatalyst was painted over carbon cloth in the form of an homogeneous dispersion prepared using Nafion® solution (5 wt%, Aldrich). After the preparation, the electrodes were hot pressed on both sides of a Nafion® 117 membrane at 125 °C for 3 min under a pressure of 247 kgf cm^{-2}. Prior to use, the membranes were exposed to KOH 6 mol L^{-1} for 24 h, as already proposed by Hou et al. [20] and Assumpção et al. [14]. The fuels, 1.0, 3.0 and 5.0 mol L^{-1} NH_4OH in 1.0 mol L^{-1} KOH were delivered at 1.0 mL min^{-1} and the oxygen flow was regulated at 150 mL min^{-1}. Polarization curves were obtained by using a potentiostat/galvanostat PGSTAT 302N Autolab.

3. Results and discussion

Fig. 1 shows the XRD patterns for PdIr/C, Pd/C and Ir/C electrocatalysts. In this Figure, it can be observed for all diffractograms a peak around $2\theta = 25°$, which is attributed to the hexagonal structure (002) of Vulcan Carbon XC-72 [8,14]. The diffraction peaks at about $2\theta = 40°, 46°, 68°$ and $82°$ on the Pd/C patterns are attributed to Pd (111), (200), (220), (311), crystalline planes, respectively, indicating a typical face-centered cubic (fcc) crystalline structure of Pd [21]. The diffraction peaks at around $2\theta = 40°, 47°, 68°$ and $82°$ on Ir/C are ascribed to Ir (111), (200), (220) and (311) crystalline planes, respectively, representing the characteristic diffraction of fcc crystalline structure of Ir [22]. It can be observed that the four diffraction peaks of PdIr/C 30:70 and 10:90 catalysts are located at higher 2θ values with respect to those of Pd/C, which can be associated to the incorporation of a lower *d* space crystal structure of Ir ($d_{111} = 2.217$) than that of Pd ($d_{111} = 2.246$), suggesting the formation of PdIr alloy [23]. For PdIr/C 50:50, 70:30 and 90:10 the diffraction peaks are only slightly shifted toward higher 2θ values with respect to those of Pd/C, indicating that some Ir atoms entered into Pd lattice and substituted Pd atoms forming also PdIr alloy. For clear observation, the magnified (111) peaks of these catalysts are inserted in Fig. 1. In all XRD patterns peaks characteristic of IrO_2 at $2\theta = 34.5°$ and $54°$ were not observed [2]. However, the presence of IrO_2 in the amorphous oxides form cannot be discarded.

The experimental compositions of all PdIr/C materials using the EDS analysis were 91:09 (nominal 90:10), 67:33 (nominal 70:30), 52:48 (nominal 50:50), 30:70 (nominal 30:70), 12:88 (nominal 10:90). As it can be seen, the real atomic ratios of each PdIr/C catalysts are close to nominal values, in all cases.

Representative TEM micrographs and histograms of particle mean diameter distribution for the binary catalysts of PdIr/C, Pd/C and Ir/C are shown in Fig. 2a–g. In all cases the particles were well dispersed on the carbon support, although some small particle agglomerations can be observed on PdIr/C 90:10 (Fig. 2b) and on PdIr/C 10:90 (Fig. 2f). The particles are with average diameter of 5.6 nm for Pd/C, 5.3 nm for PdIr/C (90:10), 5.1 nm for PdIr/C (70:30), 4.6 nm for PdIr/C (50:50), 5.0 nm for PdIr/C (30:70), 4.7 nm for PtIr/C (10:90) and 5.8 nm for Ir/C. Only Ir/C showed a small number of particles higher than 14 nm, with a maximum mean diameter of 29.8 nm. As it can be observed, the particles mean diameters are close for all materials. Additionally, from the histograms it is possible to observe that the particles distribution are really close for all binary electrocatalysts. Thus, a possible difference in the catalytic activity could be attributed to the structural characteristic of the different materials. According to the literature, it is possible to observe that materials with close particles sizes distribution and different structures and compositions show different catalytic activities for different fuels [3,24–27].

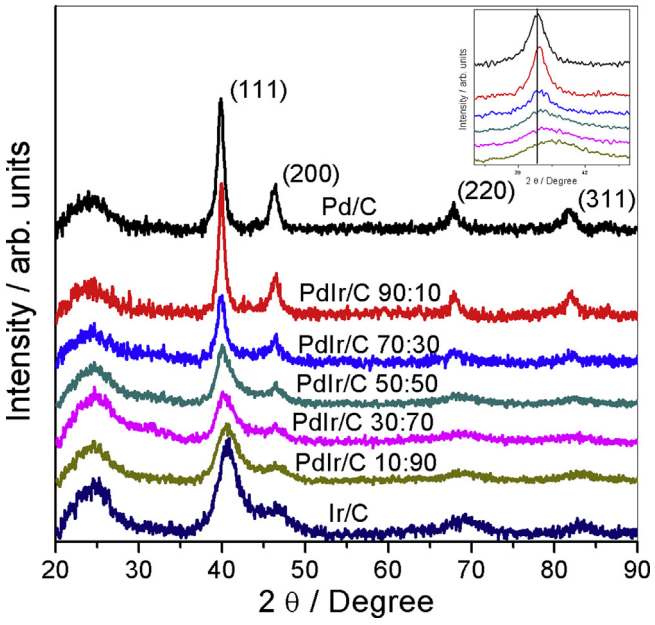

Fig. 1. X-ray diffraction patterns for the Pd/C, PdIr/C and Ir/C electrocatalysts.

The voltammograms in 1 mol L^{-1} KOH of Pd/C, PdIr/C (90:10, 70:30, 50:50, 30:70, 10:90) and Ir/C electrocatalysts between −0.85 and 0.2 V *vs.* Hg/HgO are shown in Fig. 3. It is possible to observe a typical Pd/C CV shape in alkaline media [28,29]. The potential region from −0.85 to −0.6 *vs.* Hg/HgO is associated to hydrogen adsorption/desorption on the palladium surface [29] and the hydrogen desorption is immediately followed by the adsorption of OH [28].Thus, the peak around −0.4 V *vs.* Hg/HgO is related to the OH adsorption on Pd/C [28]. The potential region from −0.25 to 0.2 V *vs.* Hg/HgO is related to the formation of palladium (II) oxide layer on the palladium surface [29]. During the reverse scan, a broad peak at about −0.2 V *vs.* Hg/HgO represents the reduction of palladium oxide layer [30].

For PdIr/C 90:10 and PdIr/C 70:30 electrocatalysts, the peak attributed to the OH adsorption on palladium (around −0.4 V vs. Hg/HgO) was not observed, which can be associated to the presence of iridium. Moreover, the peak corresponding to palladium oxide reduction at about −0.2 V *vs.* Hg/HgO is in small intensities if compared to the Pd/C. This difference can be explained due to the presence of iridium. The changes on palladium profile obtained from CV in alkaline media were also reported in the literature using PdAu/C 30:70 [29], PdSn/C and PdRuSn/C [30].

In the Ir/C voltammogram the hydrogen region is well defined between −0.85 V and −0.6 V vs. Hg/HgO, as observed in the literature [8]. Considering the PdIr/C 10:90, PdIr/C 30:70 and PdIr/C 50:50 profiles, they are very similar to Ir/C, this can probably be related to the high amount of iridium in these compositions.

Fig. 4 shows the voltammograms of Pd/C, PdIr/C (90:10, 70:30, 50:50, 30:70, 10:90) and Ir/C electrocatalysts in 1 mol L^{-1} KOH + 1 mol L^{-1} NH_4OH. As it can be observed, Ir/C showed a similar shape when compared to the ones reported in the literature [5,8,31]. The presence of ammonia in the KOH solutions changes the shape of the hydrogen upd region indicating that ammonia is adsorbed on iridium in this potential interval [31]. The oxidation peak at around −0.29 V *vs.* Hg/HgO can be associated with ammonia oxidation to N_2, since, as reported by Vooys et al. [31] at a potential below −0.05 V *vs* Hg/HgO the selectivity to N_2 is 100% in iridium electrodes.

Using PdIr/C 10:90 and PdIr/C 30:70 electrocatalysts the ammonia oxidation peak is shifted 10 mV to lower values (−0.3 V *vs.* Hg/HgO) in comparison to Ir/C. Moreover, the peak current density is 1.3 and 1.7 times higher using PdIr/C 10:90 and PdIr/C 30:70 than that obtained for the same process using Ir/C, respectively. It is important to stress that the onset potential for ammonia electro-oxidation is lower on PdIr/C 30:70 (~−0.53 V *vs.* Hg/HgO) than on PdIr/C 10:90 (~−0.51 V vs. Hg/HgO) and Ir/C (~−0.49 V vs. Hg/HgO). This phenomenon could be associated to the presence of palladium, since the ammonia electro-oxidation starts in lower potentials on this metal than on iridium [8,31].

Considering the PdIr/C 50:50 and the PdIr/C 70:30 electrocatalysts, the onset potential for ammonia electro-oxidation is around −0.53 V *vs.* Hg/HgO. From the voltammograms it is possible to observe that the peak current density is shifted to lower potential when compared to Ir/C, PdIr/C 10:90 and PdIr/C 30:70 (~−0.32 V and ~−0.33 V *vs.* Hg/HgO, respectively). As

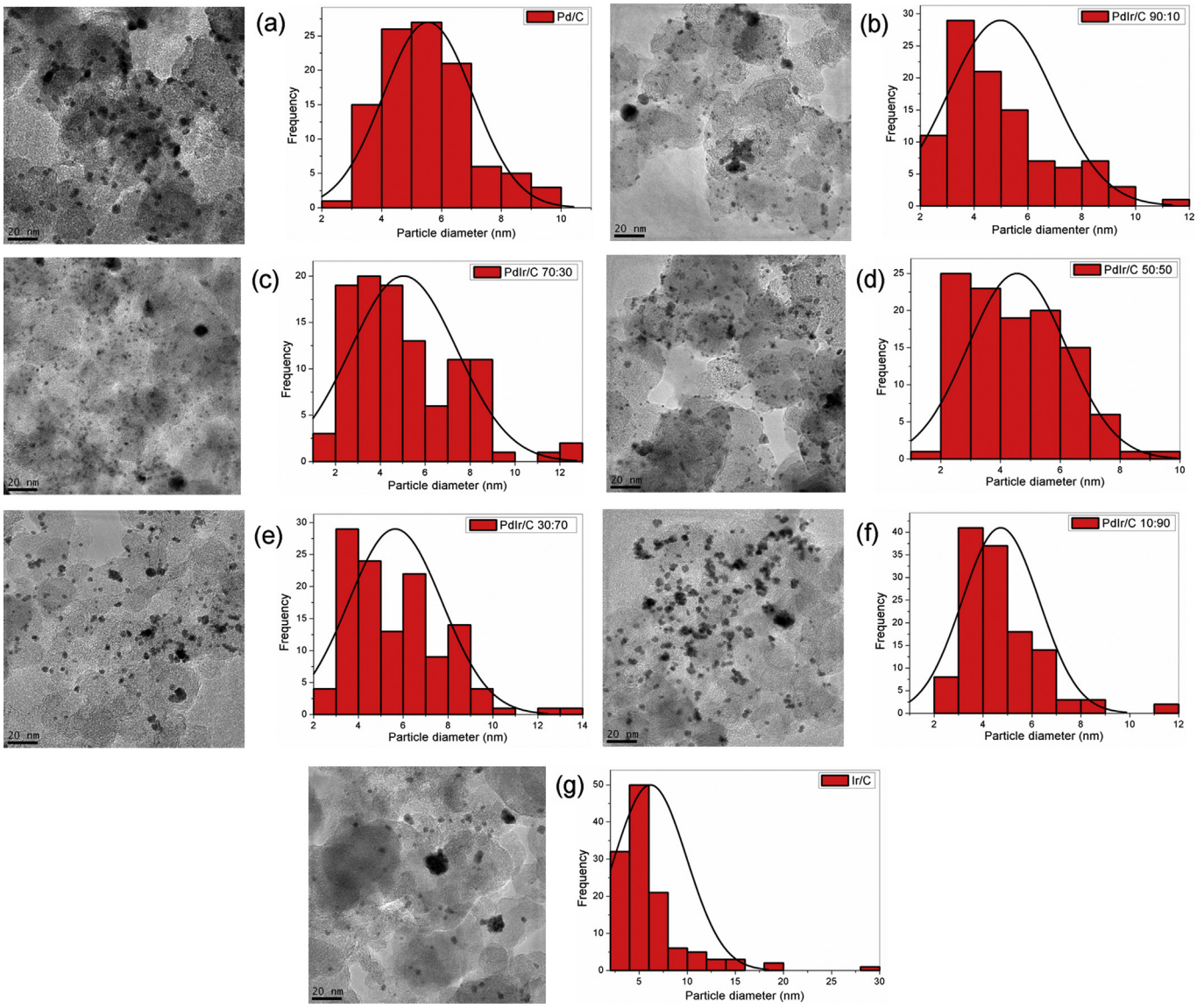

Fig. 2. TEM micrographs and histograms of (a) Pd/C, (b) PdIr/C 90:10, (c) PdIr/C 70:30, (d) PdIr/C 50:50, (e) PdIr/C 30:70, (f) PdIr/C 90:10 and (g) Ir/C.

already mentioned before, this might be related to the presence of palladium on the electrocatalysts compositions. It is also possible to observe that increasing the palladium content on PdIr/C compositions there is also a shift on the peak current density to lower potential values. Lomocso and Baranova [8] reported that the introduction of palladium on platinum electrocatalysts, also shifted the ammonia oxidation peak to lower potential when compared to Pt/C.

The voltammogram of ammonia electro-oxidation on Pd/C has a different shape than those obtained for Ir/C and PdIr/C binary electrocatalysts. Using Pd/C there is clearly two processes in ammonia oxidation reaction. The onset potential of the first process starts at about −0.55 V *vs.* Hg/HgO, yielding a peak current density at −0.38 V *vs.* Hg/HgO, a peak for ammonia electro-oxidation on palladium around −0.38 V *vs.* Hg/HgO was also observed by Vooys et al. [31]. It is important to stress that both, the onset potential and also the peak current density for ammonia oxidation on Pd/C first process, are shifted to lower potential values when compared for the same process using Ir/C and all PdIr/C materials. In fact, this could be explained since the Pd dehydrogenates ammonia at lower overpotential [8,31]. Another interesting point is that this process occurs at the same region of OH adsorption on palladium (around −0.4 V *vs.* Hg/HgO), and one plausible explanation for this peak is that the OH species are reacting with dehydrogenated ammonia species forming nitrogen oxygenated species, since palladium is not selective for ammonia oxidation to N_2 [8,31]. Another important point to stress is that in the potential window at about −0.4 V to −0.2 V vs. Hg/HgO, the electrode deactivate, indicating the poisoning of the electrocatalyst surface.

The second process for ammonia electro-oxidation on Pd/C starts at about −0.2 V *vs.* Hg/HgO a region related to the palladium (II) formation of oxide layer on the palladium surface. Thus, dehydrogenated nitrogen species probably are oxidized to nitrogen oxide species on the oxide layer on palladium surface, since as it has been already mentioned above, palladium is not selective for N_2 and then nitrogen oxide species such as N_2O can be formed as already proposed by Vooys at al. [31].

Among the PdIr/C materials, PdIr/C 90:10 shows poor electrocatalytic activity toward ammonia electro-oxidation. Analyzing the ammonia oxidation with this material, it is possible to observe that

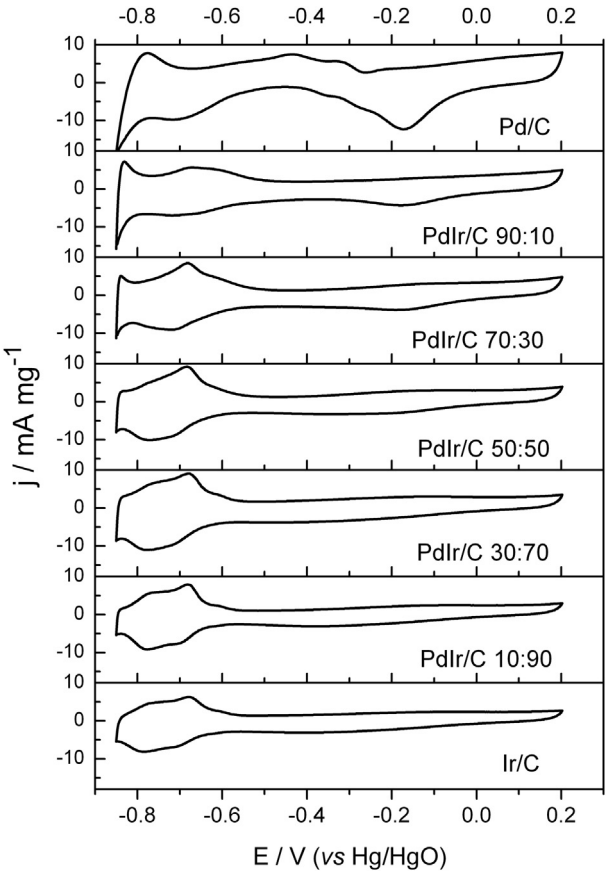

Fig. 3. Voltammograms of Pd/C, PdIr/C and Ir/C electrocatalysts in 1 mol L^{-1} KOH at $\nu = 20$ mV s^{-1}.

there is a peak with low intensity at −0.34 V *vs.* Hg/HgO and a second one at −0.1 V *vs.* Hg/HgO. This second process could be associated to the high amount of palladium on its composition. However, the presence of only 10% of iridium on its composition promotes a great change in the voltammogram profile, and do not promotes good electrocatalytic activity.

Fig. 5 shows the chronoamperometric curves for 1 mol L^{-1} NH_4OH + 1 mol L^{-1} KOH electro-oxidation on Pd/C, PdIr/C (90:10, 70:30, 50:50, 30:70, 10:90) and Ir/C electrocatalysts, obtained by polarization at −0.35 V *vs.* Hg/HgO. In order to investigate the electrocatalysts stability these measurements were carried out for 5 h.

As it can be observed in all chronoamperometric curves, the current decreases continuously within the first hour, and after the second hour, the fall is less pronounced, excepted for Pd/C and PdIr/C 90:10 that deactivates in only 50 and 820 s, respectively. For these two electrocatalysts the current drops below zero. This fact can be probably associated to palladium surface poisoning by N_{ads}, [8,31].

It is important to stress that the maximum peak current density for ammonia electro-oxidation on Pd/C is in lower overpotential (−0.38 V *vs.* Hg/HgO) than the one used for chronoamperometric measurements (−0.35 V *vs.* Hg/HgO). However, chronoamperometric experiments at −0.38 V were also performed when compared to that obtained at −0.35 V vs. Hg/HgO.

Taking into account the chronoamperometric results, the highest current density during 5 h experiment was obtained using PdIr/C 30:70 while the PdIr/C 10:90 was the second promisor material. This probably can be related to an enhanced synergic effect between iridium and small amounts of palladium in PdIr/C

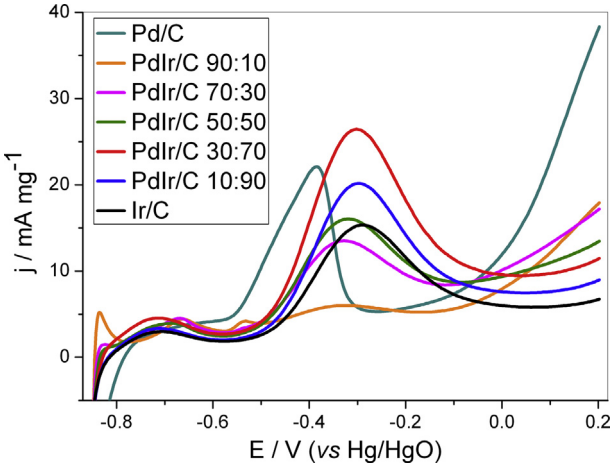

Fig. 4. Voltammograms of Pd/C, PdIr/C and Ir/C electrocatalysts in 1 mol L^{-1} KOH + 1 mol L^{-1} NH_4OH at $\nu = 20$ mV s^{-1}.

alloy. Lomocso and Baranova [8] performed experiments with Pt/C, PtIr/C, PtSnOx/C and PtPd/C toward ammonia electro-oxidation and reported that PtPd/C 70:30 showed higher catalytic activity than Pt/C. Therefore, they showed that lower amounts of palladium on PtPd/C alloys also improve the catalytic activity for ammonia electro-oxidation as obtained for PdIr/C 30:70 in the present study.

PdIr/C 50:50 shows superior initial current density than Ir/C (see insert in the Fig. 5), however, this material has lower stability than Ir/C and the current density after 5 h is lower than the obtained for Ir/C. This can be related to the easily poisoning of PdIr/C 50:50 when compared to Ir/C. The same occurs on PdIr/C 70:30 electrocatalyst. This can be probably associated to the high percentage of palladium in its compositions. Similar results were obtained by Lomosco and Baranova toward ammonia electro-oxidation on PtPd/C 50:50 and Pt/C, in which these two materials show almost the same behavior in chronoamperometric experiments [8].

Fig. 6 shows the polarization and power density curves for 1.0, 3.0 and 5.0 NH_4OH mol L^{-1} in KOH 1 mol L^{-1} using Pd/C, PdIr/C (90:10, 70:30, 50:50, 30:70, 10:90) and Ir/C catalysts as anode in a DAFC operated at 40 °C and Pt/C BASF catalysts as cathode in all

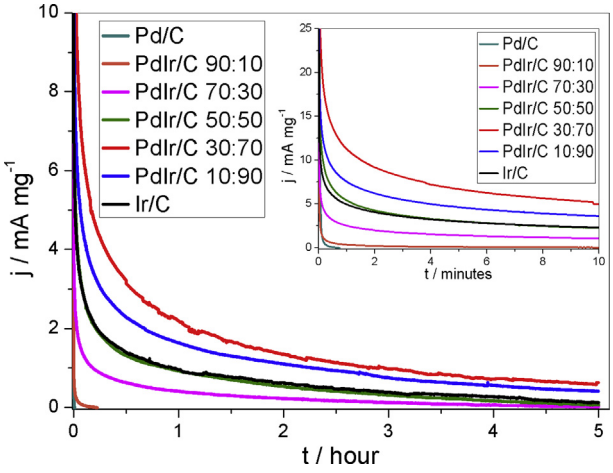

Fig. 5. Chronoamperometric measurements at −0.35 V *vs.* Hg/HgO for Pd/C, PdIr/C and Ir/C electrocatalysts in 1 mol L^{-1} KOH + 1 mol L^{-1} NH_4OH. Insert the first 10 min of the experiments.

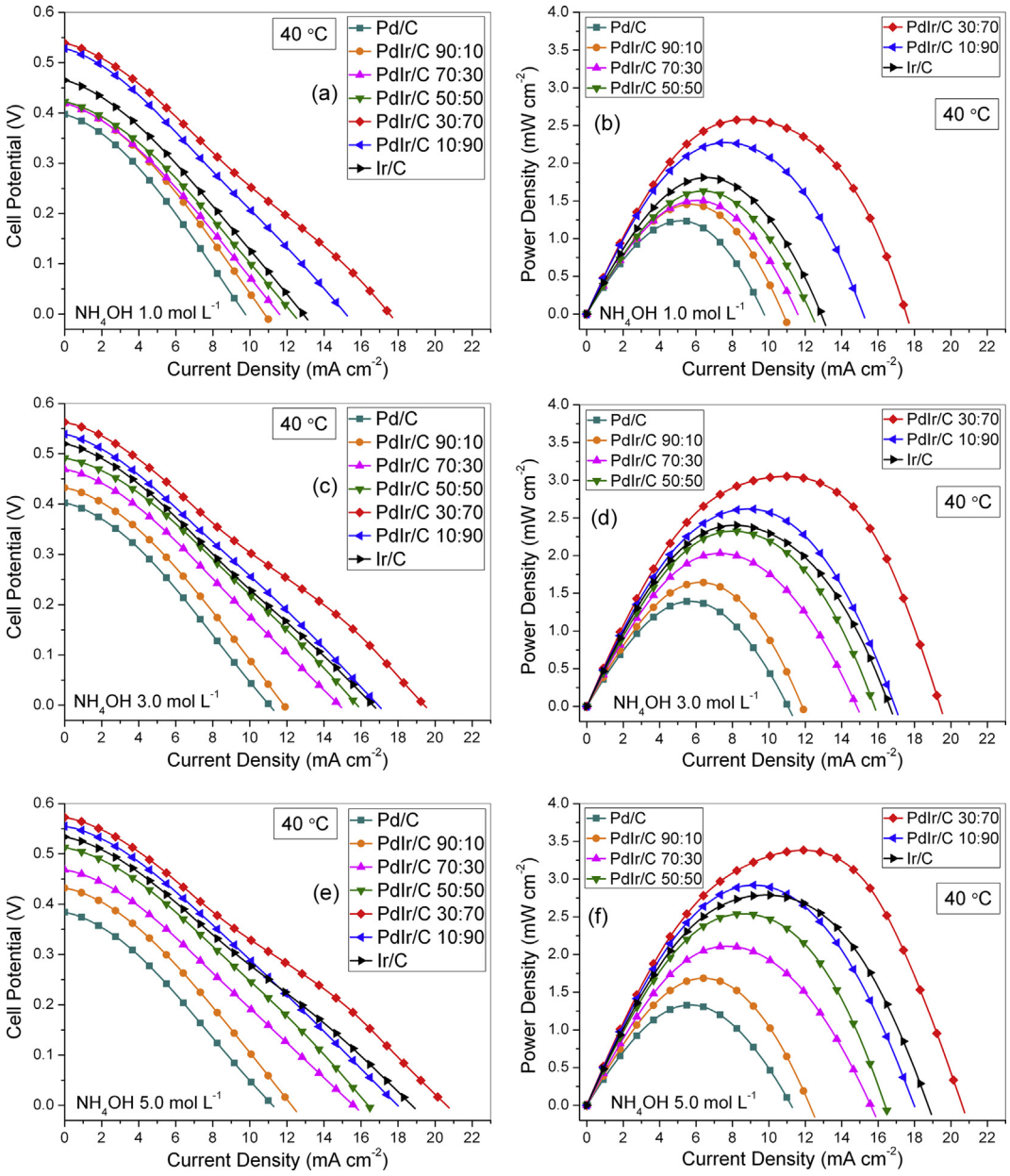

Fig. 6. Polarization and power density curves of a 5 cm^2 DAFC at 40 °C. (a) and (b) using NH_4OH 1.0 mol L^{-1} (c) and (d) using NH_4OH 3.0 mol L^{-1}(e) and (f) using NH_4OH 5.0 (both in KOH 1 mol L^{-1}), 2 mg metal cm^{-2} in both anode and cathode. Pt/C BASF was used as cathode in all experiments.

experiments. The performance of each catalyst was improved as NH_4OH concentration increases, except for Pd/C and PdIr/C (90:10) (see Table 1 and Table 2). It is possible to observe that by using PdIr/C 30:70, best results were achieved. Using PdIr/C 30:70, the maximum power density was 52%, 54% and 60% higher than that for Pd/C in NH_4OH 1.0 mol L^{-1}, NH_4OH 3.0 mol L^{-1} and NH_4OH 5.0 mol L^{-1}, respectively. When the same comparison was made with Ir/C these values are between 18% and 30%.

Table 1
Obtained open circuit potential for DAFC experiments at 40 °C and 50 °C.

NH_4OH concentrations	Operation temperature	Electrocatalysts compositions						
		Pd/C	PdIr/C 90:10	PdIr/C 70:30	PdIr/C 50:50	PdIr/C 30:70	PdIr/C 10:90	Ir/C
		OCV/V						
1 mol L^{-1}	40 °C	0.397	0.419	0.419	0.423	0.539	0.528	0.465
	50 °C	0.384	0.415	0.419	0.425	0.548	0.540	0.487
3 mol L^{-1}	40 °C	0.402	0.433	0.469	0.492	0.563	0.539	0.520
	50 °C	0.394	0.426	0.454	0.500	0.565	0.563	0.529
5 mol L^{-1}	40 °C	0.384	0.432	0.468	0.513	0.573	0.555	0.534
	50 °C	0.376	0.424	0.460	0.528	0.576	0.564	0.536

Table 2
Maximum power density obtained for DAFC experiments at 40 °C and 50 °C.

NH_4OH concentrations	Operation temperature	Electrocatalysts compositions						
		Pd/C	PdIr/C 90:10	PdIr/C 70:30	PdIr/C 50:50	PdIr/C 30:70	PdIr/C 10:90	Ir/C
		Power density/mW cm^{-2}						
1 mol L^{-1}	40 °C	1.235	1.454	1.508	1.631	2.579	2.271	1.811
	50 °C	1.327	1.602	1.763	1.811	3.064	2.710	2.239
3 mol L^{-1}	40 °C	1.394	1.423	2.028	2.325	3.052	2.620	2.401
	50 °C	1.495	1.765	2.141	2.647	3.528	2.937	2.928
5 mol L^{-1}	40 °C	1.327	1.681	2.109	2.540	3.381	2.919	2.788
	50 °C	1.484	1.776	2.331	3.007	3.707	3.192	3.220

Actually, using Pd/C the worst results were obtained, this phenomenon probably is related to the surface poisoning of Pd by N_{ads}. Furthermore, using NH_4OH 5.0 mol L^{-1}, both open circuit potential and maximum power density were lower if compared to NH_4OH 3.0 mol L^{-1}, this can be explained since the rate of N_{ads} formation increases in NH_4OH 5.0 mol L^{-1} concentration thereby, blocking active sites. It was reported that because of high N_{ads}-Pd binding energy, Pd exhibits a very low catalytic activity for ammonia

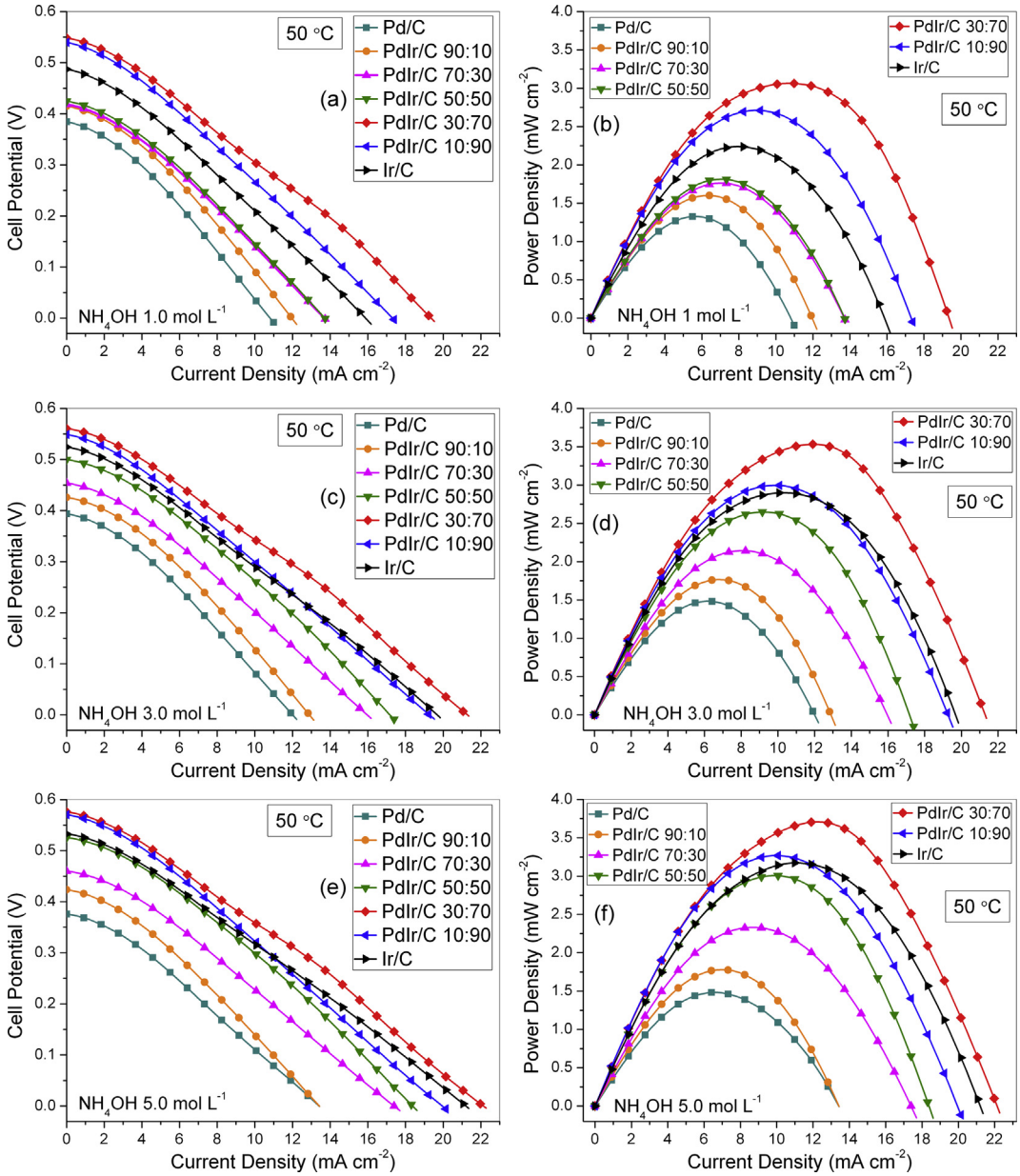

Fig. 7. Polarization and power density curves of a 5 cm^2 DAFC at 50 °C. (a) and (b) using NH_4OH 1.0 mol L^{-1} (c) and (d) using NH_4OH 3.0 mol L^{-1}(e) and (f) using NH_4OH 5.0 (both in KOH 1 mol L^{-1}), 2 mg metal cm^{-2} in both anode and cathode. Pt/C BASF was used as cathode in all experiments.

electro-oxidation in KOH solution [6]. This result is in agreement to the one obtained on chronoamperometric experiments. In both experiments Pd/C shows very low catalytic activity.

It can also be seen from Fig. 6 that the highest open circuit potential (0.573 V) was obtained using PdIr/C 30:70 and NH_4OH 5 mol L^{-1}. It is important to stress that the open circuit potential and the maximum power density improved with the iridium addition until 70% in the PdIr/C catalysts. Similar results were obtained for PtIr/C catalysts [6].

The best results obtained using PdIr/C 30:70 and 10:90 binary composition could be explained because palladium sites dehydrogenate ammonia at lower overpotential and associated to it, the lower N_{ads}-Ir binding energy when compared to N_{ads}-Pd [6,8], contributes to the lower surface coverage by N_{ads} on PdIr/C. Thus, the enhanced synergic effect between palladium and iridium was obtained using PdIr/C 30:70. Additionally, the electronic effect generated between two metals in the alloy nanoparticles might also be responsible for the increase in the catalytic activity of PdIr/C catalysts, since it causes the weakness of the adsorption strength of poisonous N_{ads} intermediate, facilitating the ammonia oxidation [8,14]. On the other hand, using PdIr/C 50:50, 70:30 and 90:10, the results were lower than those obtained using Ir/C, probably due to the higher amounts of palladium in these proportions, since as already explained, palladium is easily poisoning by N_{ads}.

The experiments were also performed at 50 °C. Fig. 7 show the polarization and the power density curves for 1.0, 3.0 and 5.0 NH_4OH mol L^{-1} in KOH 1 mol L^{-1} using Pd/C, PdIr/C and Ir/C electrocatalysts as anode in a DAFC and Pt/C BASF electrocatalysts as cathode in all experiments.

As obtained at 40 °C, the open circuit potential and the maximum power density increases as follows: Pd/C < PdIr/C 90:10 < PdIr/C 70:30 < PdIr/C 50:50 < Ir/C < PdIr/C 10:90 < PdIr/C 30:70. Comparing the maximum power density obtained with each catalyst and the two different temperatures it is possible to observe that the higher values were obtained at 50 °C (see Table 2). This result is probably related to the increased of the kinetics for ammonia electro-oxidation when the temperature increases, as also observed for ethanol oxidation [29,32]. Therefore, based on the results obtained in this study, better results are obtained when the DAFCs is operated at 50 °C instead of 40 °C.

4. Conclusions

Among the PdIr/C materials studied considering electrochemical and also DAFC experiments, the highest current density, power density and open circuit potential was obtained using PdIr (30:70). The maximum power density obtained with PdIr/C 30:70 using 5 mol L^{-1} NH_4OH and 1 mol L^{-1} KOH at 40 °C is 60% and 30% higher than the one obtained with Pd/C and Ir/C, respectively.

The best result observed with this material can be associated to the electronic effect between Pd and Ir in alloyed state associated to the enhanced synergic effect in these specific atomic ratio assigned to Pd sites that dehydrogenate ammonia at lower overpotential. Additionally, the best results obtained when operating the DAFC at 50 °C instead of 40 °C could be related to the increased kinetic of ammonia electro-oxidation when the temperature increases.

Acknowledgments

The authors wish to thank FAPESP (2013/01577-0, 2011/18246-0, 2012/22731-4, 2012/03516-5), CNPq (150639/2013-9, 141469/2013-7, 474913/2012-0, 406612/2013-7) and INCT Instituto Nacional de Ciência e Tecnologia (INCT) Energia e Meio Ambiente (Process Number: 573.783/2008-0) for the financial support.

References

[1] C. Zamfirescu, I. Dincer, Fuel Process. Technol. 90 (2009) 729–737.
[2] J.C.M. Silva, B. Anea, R.F.B. De Souza, M.H.M.T. Assumpcao, M.L. Calegaro, A.O. Neto, M.C. Santos, J. Braz. Chem. Soc. 24 (2013) 1553–1560.
[3] S.C. Zignani, V. Baglio, J.J. Linares, G. Monforte, E.R. Gonzalez, A.S. Aricò, Electrochim. Acta 70 (2012) 255–265.
[4] S. Suzuki, H. Muroyama, T. Matsui, K. Eguchi, J. Power Sources 208 (2012) 257–262.
[5] F.J. Vidal-Iglesias, J. Solla-Gullón, V. Montiel, J.M. Feliu, A. Aldaz, J. Power Sources 171 (2007) 448–456.
[6] C. Zhong, W.B. Hu, Y.F. Cheng, J. Mater. Chem. A 1 (2013) 3216–3238.
[7] A. Allagui, M. Oudah, X. Tuaev, S. Ntais, F. Almomani, E.A. Baranova, Int. J. Hydrogen Energy 38 (2013) 2455–2463.
[8] T.L. Lomocso, E.A. Baranova, Electrochim. Acta 56 (2011) 8551–8558.
[9] A. Allagui, S. Sarfraz, E.A. Baranova, Electrochim. Acta 110 (2013) 253–259.
[10] B.K. Boggs, G.G. Botte, Electrochim. Acta 55 (2010) 5287–5293.
[11] F.J. Vidal-Iglesias, N. Garcıa-Aráez, V. Montiel, J.M. Feliu, A. Aldaz, Electrochem. Commun. 5 (2003) 22–26.
[12] A. Brouzgou, S.Q. Song, P. Tsiakaras, Appl. Catal. B Environ. 127 (2012) 371–388.
[13] R. Lan, S. Tao, Electrochem. Solid State Lett. 13 (2010) B83–B86.
[14] M.H.M.T. Assumpção, S.G. da Silva, R.F.B. de Souza, G.S. Buzzo, E.V. Spinacé, A.O. Neto, J.C.M. Silva, Int. J. Hydrogen Energy.
[15] R.S. Henrique, R.F.B. De Souza, J.C.M. Silva, J.M.S. Ayoub, R.M. Piasentin, M. Linardi, E.V. Spinace, M.C. Santos, A.O. Neto, Int. J. Electrochem. Sci. 7 (2012) 2036–2046.
[16] A.O. Neto, M.M. Tusi, N.S. de Oliveira Polanco, S.G. da Silva, M. Coelho dos Santos, E.V. Spinacé, Int. J. Hydrogen Energy 36 (2011) 10522–10526.
[17] T. Herranz, S. García, M.V. Martínez-Huerta, M.A. Peña, J.L.G. Fierro, F. Somodi, I. Borbáth, K. Majrik, A. Tompos, S. Rojas, Int. J. Hydrogen Energy 37 (2012) 7109–7118.
[18] R.F.B. Souza, G.S. Buzzo, J.C.M. Silva, E.V. Spinacé, A.O. Neto, M.H.M.T. Assumpção, Electrocatalysis (2014) 1–7.
[19] J.C.M. Silva, R.F.B. Souza, G.S. Buzzo, E.V. Spinacé, A.O. Neto, M.H.M.T. Assumpção, Ionics (2014) 1–8.
[20] H. Hou, S. Wang, W. Jin, Q. Jiang, L. Sun, L. Jiang, G. Sun, Int. J. Hydrogen Energy 36 (2011) 5104–5109.
[21] G. Li, L. Jiang, Q. Jiang, S. Wang, G. Sun, Electrochim. Acta 56 (2011) 7703–7711.
[22] J. Tayal, B. Rawat, S. Basu, Int. J. Hydrogen Energy 36 (2011) 14884–14897.
[23] S.Y. Shen, T.S. Zhao, J.B. Xu, Electrochim. Acta 55 (2010) 9179–9184.
[24] J.C.M. Silva, L.S. Parreira, R.F.B. De Souza, M.L. Calegaro, E.V. Spinacé, A.O. Neto, M.C. Santos, Appl. Catal. B Environ. 110 (2011) 141–147.
[25] J.C.M. Silva, R.F.B. De Souza, L.S. Parreira, E.T. Neto, M.L. Calegaro, M.C. Santos, Appl. Catal. B Environ. 99 (2010) 265–271.
[26] J. Ribeiro, D.M. dos Anjos, K.B. Kokoh, C. Coutanceau, J.M. Léger, P. Olivi, A.R. de Andrade, G. Tremiliosi-Filho, Electrochim. Acta 52 (2007) 6997–7006.
[27] E. Antolini, J.R.C. Salgado, E.R. Gonzalez, J. Electroanal. Chem. 580 (2005) 145–154.
[28] L. Ma, D. Chu, R. Chen, Int. J. Hydrogen Energy 37 (2012) 11185–11194.
[29] A.N. Geraldes, D.F. da Silva, E.S. Pino, J.C.M. da Silva, R.F.B. de Souza, P. Hammer, E.V. Spinacé, A.O. Neto, M. Linardi, M.C. dos Santos, Electrochim. Acta 111 (2013) 455–465.
[30] R.M. Modibedi, T. Masombuka, M.K. Mathe, Int. J. Hydrogen Energy 36 (2011) 4664–4672.
[31] A.C.A. de Vooys, M.T.M. Koper, R.A. van Santen, J.A.R. van Veen, J. Electroanal. Chem. 506 (2001) 127–137.
[32] L. Jiang, A. Hsu, D. Chu, R. Chen, Int. J. Hydrogen Energy 35 (2010) 365–372.